

Miscibility and Crystallization Behavior of Poly(ethylene-*co*-vinylalcohol)/Poly(maleic anhydride-*alt*-ethylene) Blend

Taieb Aouak, Abdullah Saad AlArifi, Mohamed Ouladsmane

Chemistry Department, College of Science, King Saud University, Riyadh 11459, Saudi Arabia

Received 4 July 2010; accepted 4 November 2011

DOI 10.1002/app.36470

Published online 20 January 2012 in Wiley Online Library (wileyonlinelibrary.com).

ABSTRACT: The miscibility of poly(vinylalcohol-*co*-ethylene) (PEVA) with poly(ethylene-*alt*-maleic anhydride) (PEMAH) blends was investigated over a wide range of compositions by viscosimetry and DSC analyses using Krigbaum–Wall and Kwei approaches. The results revealed that the blends were completely miscible in all proportions due to the specific interactions between the hydroxyl groups of PEVA and the carbonyl groups of PEMAH. From Nishi equation, the interaction parameter of Flory was found to be -0.89 . The nonisothermal crystallization behavior and kinetics of this system were also investigated and compared with those of the pure PEVA.

There were strong dependencies of the degree of crystallinity (X_T), peak crystallization temperature (T_p), half time of crystallization ($t_{1/2}$), and Ozawa exponent (m) on PEMAH content and cooling rate. The crystallization activation energy (E_c) that was calculated from Kissinger model increased with increasing PEMAH composition in the blend. © 2012 Wiley Periodicals, Inc. *J Appl Polym Sci* 125: 2262–2270, 2012

Key words: miscibility; poly(vinylalcohol-*co*-ethylene); poly(ethylene-*alt*-maleic anhydride); nonisothermal crystallization; viscosimetry

INTRODUCTION

Recently, poly(vinylalcohol-*co*-ethylene) (PEVA) membranes have attracted the research interest in the fields of biomedical science and water treatment process, because of their good blood compatibility and hydrophilicity.^{1,2} PEVA has been widely used as a food packing material because of its excellent gas barrier properties and harmlessness to health. PEVA in different compositions is essentially random and semicrystalline over the entire range of composition in spite of the irregularity and nonsteriospecificity of vinyl alcohol units distributed in the copolymer chain.³ Nevertheless, PEVA copolymers have several problems associated with its processing; like deficient thermoformability and limited miscibility with other polymers due to the high density of hydrogen bonding between the hydroxyl groups.³ Miscible blends of PEVA have a lower critical solution temperature (LCST) behavior and phase separation anticipated at processing temperatures. However, PEVA after blending with other polymers can offer opportunities to extend and explore their many useful interesting properties and to modify their undesirable properties. Several investigations

were reported on the miscibility of these copolymers with other polymers using different techniques, for example, with nylon 6–12,⁴ poly(4-vinylpyridine-*co*-styrene) (PVPST),⁵ poly(*N,N*-dimethylacrylamide) (PDMA),⁶ poly(ethyloxazoline) (PEOX),⁷ poly(vinylpyrrolidone) (PVP),⁸ poly(propylene),⁹ poly(L-lactic acid),¹⁰ polyamide-6 (PA-6),¹¹ acetylated starch (TPAS),¹² aromatic copolyester (PETG),¹³ and recently poly(methylmethacrylate) (PMMA).¹⁴

Miscibility was evident in blends with nylon 6–12, PVP, PBMA, PA6–12, PA-6, and TPAS,^{4,8,10–12} which could be attributed to the hydrogen bonding involving hydroxyl groups of PEVA and electron donor groups of the other polymer. The blending of PEVA with PVPST, PDMA, and PEOX^{5–7} were partially miscible depending on the composition of comonomer ethylene in PEVA. The other blends cited above^{9,13,14} were thermodynamically immiscible and in some cases a compatibilizer was used to achieve the desired properties of the blends.

Blends based on polyolefins have been compatibilized by reactive extrusion, where functionalized polyolefins are used to form copolymers at the interface to improve the compatibility between the components and the adhesion between the phases. Maleic anhydride grafted polyolefins are the most useful blends for the above purpose.^{15–17}

The potential of this type of functionalized polymers is to provide an amphiphilic polymeric ionomers as candidates for drug controlled release, based on

Correspondence to: T. Aouak (t.aouak@yahoo.fr).

TABLE I
Intrinsic Viscosities and Viscosimetric Interaction Parameters of Different PEVA/PEMAH Blends

System, PEVA/PEMAH	b_{ii}	b_m	b_{23}^{exp}	b_{23}^{th}	Δb_{23}	$[\eta]^{\text{exp}}$	$[\eta]^{\text{cal}}$
100 : 0	0.362	–	–	–	–	0.963	–
90 : 10	–	0.382	0.483	0.288	0.195	1.143	0.945
75 : 25	–	0.422	0.544	0.288	0.256	1.038	0.917
50 : 50	–	0.482	0.668	0.288	0.380	0.962	0.871
25 : 75	–	0.450	0.464	0.288	0.507	0.865	0.824
10 : 90	–	0.234	0.945	0.288	0.657	0.862	0.796
0 : 100	0.230	–	–	–	–	0.778	–

their biocompatibility.¹⁸ No doubt, the utilization of blending PEVA with PEMAH would be increased in the different domains cited above.

To achieve this goal, we have studied the miscibility of PEVA/PEMAH blends and the effects of amorphous PEMAH on the crystallization of PEVA in PEVA/PEMAH blends by differential scanning calorimetry (DSC) and the miscibility of this system was confirmed using the viscosimetry method. The nonisothermal crystallization kinetics of PEVA and the PEVA/PEMAH blends at different compositions were also studied.

EXPERIMENTAL

Materials

The polymers used in this work, poly(ethylene-co-vinylalcohol) (PEVA) (contained 38 mol % of ethylene unit) and poly(maleic anhydride-*alt*-ethylene) (PEMAH) were purchased from Aldrich. The number average molecular weights are 29,000 and 100,000, respectively. The PEVA/PEMAH blends were prepared by solution casting from *N,N*-dimethylformamide (DMF) by slow evaporation at 60°C for 1 week; then it was kept at 80°C under vacuum for 1 month, to remove DMF completely.

Differential scanning calorimeter

The glass transition temperature of the pure components and the blends were measured by DSC (Setaram Labsys DSC 16), previously calibrated with indium. Samples weighing between 10 and 12 mg were packed in aluminum DSC pans before placing in DSC cell. The samples were heated from 30 to 240°C at a heating rate of 20°C min⁻¹ and kept at 200°C for 10 min to destroy any nuclei that might act as a crystal seed. The samples were then cooled down to 30°C at constant rates of 5, 10, 20, 30, and 40°C min⁻¹, respectively. For uniform thermal history in all samples, the thermograms have been represented by the results of the second run, after quenching just above the T_g . No degradation phenomena of PEVA, PEMAH, and PEVA/PEMAH blends were observed in all thermograms. This

finding was also confirmed by a test of solubility realized after DSC analysis. The glass transition temperature was taken at the midpoint in the heat capacity change with temperature. The melting and crystallization points were taken at the summits of the peaks.

Viscosimetry

The reduced viscosity measurements of PEVA, PEMAH, and their blends were realized at 30°C in DMF using a viscosimeter Ubbelohde Scott Gerate type Avs 310. The description of the technique used and methods of measurement have been detailed by Soria et al.¹⁹ The specific and intrinsic coefficients of each copolymer viscosity in the DMF/polymeric binary or DMF/copolymer/copolymer ternary systems have been determined by infinite-dilution extrapolation of the copolymer with the DMF/polymer binary mixture, i.e., if the system is a named solvent (S)/copolymer(Cx)/copolymer(Cy), the values of the intrinsic coefficient of viscosity of copolymer (Cx) in a dilute solution of polymer (Cy) were obtained by zero-concentration extrapolation of Cx in a binary mixture, in which the concentration of Cx was constant.

RESULTS AND DISCUSSION

The study of the miscibility by viscosimetry

To prove the miscibility of our system, at ambient temperature (30°C), we have determined the viscosimetric parameters of a ternary system composed of a solvent (1) and two polymers, (2) and (3), at different proportions and resorted to Krigbaum–Wall approach.²⁰ According to this approach, a mixture of two polymers is miscible when the value of the viscosimetric interaction between polymer (2) and polymer (3) (Δb_{23}) is positive.

Table I summarizes the intrinsic viscosities ($[\eta]$) of copolymers and their blends in DMF at 30°C. The experimental viscosimetric parameters between polymer (2) and polymer (3) (b_{23}^{exp}), the theoretical values (b_{23}^{th}) and their differences (Δb_{23}) were determined according to the Krigbaum–Wall approach.

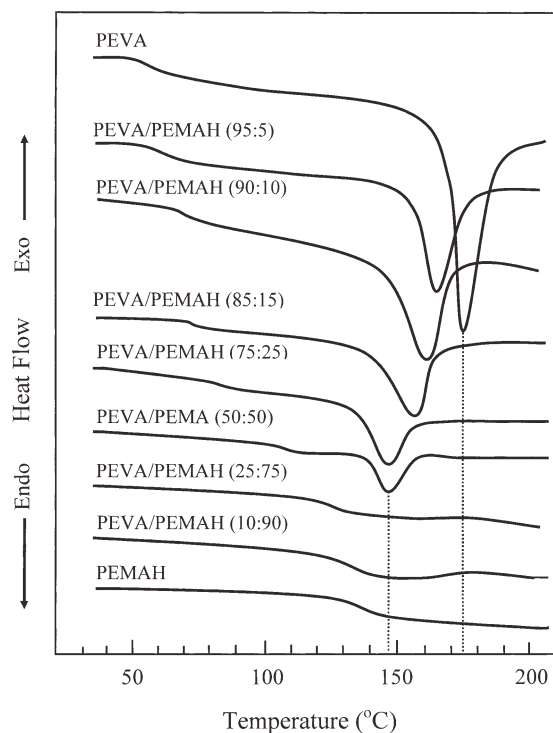


Figure 1 The DSC thermograms of PEVA, PEMA, and their blends at different compositions in wt %.

These results confirmed the perfect miscibility of PEVA/PEMAH blend in all proportions as the positive Δb_{23} values indicate. It was also observed that, the Δb_{23} increased with increasing the PEMAH content. According to different authors,^{21,22} the negative deviation of the experimental intrinsic viscosities ($[\eta]^{\text{exp}}$) from those calculated from the weight average of the intrinsic viscosities of the pure constituents ($[\eta]^{\text{cal}}$) can be explained by the predominance of heterogenic contacts (segments of polymer (*i*)-segment of polymer (*j*) of different types) on the homogenic contacts (segments of polymer (*i*)-segment of polymer (*i*) of the same type). This difference is attributed in this case to the hydrogen bond interactions between the PEVA hydroxyl group and the PEMAH carbonyl group.

Blend appearance

The cast-film samples of all PEVA/PEMAH compositions were apparently clear and homogeneous above the equilibrium melting point T_m of PEVA. When observed through an optical microscope, the blend films were completely free of any haziness or heterogeneous domains. The effects of morphology on the crystallization behavior of PEVA in the blends will be discussed later.

The study of the miscibility by DSC

DSC analysis was performed on the samples to reveal their glass-transition behavior. Figure 1 shows

that the thermograms exhibited one apparent T_g for PEVA/PEMAH blends within a wide range of compositions, as indicated in the curves. All thermograms clearly showed that there was a single T_g corresponding to each composition and the values of T_g were composition dependent. By applying the conventional T_g criterion for determining phase miscibility, the blend was apparently miscible in the amorphous fraction. Utracki et al.²³ concluded that the use of T_g in the examination of polymer-polymer miscibility is based on the premise that a single T_g indicates that the domain size is below 15 nm. Therefore, only a single T_g blend indicates the miscibility between PEVA and PEMAH on scale of 15 nm. The T_g and T_m values of the copolymers and their blends are gathered in Table II. With reference to these results, it was noted that the T_g (onset) of the blends initially increased slightly then increased significantly with increasing PEMAH fraction in the PEVA/PEMAH blend. These thermograms are also showing an important depression in the melting temperature of PEVA with an increase in PEMAH content, which indicated that the crystallinity of PEVA decreased in the blends. The melting temperature (T_m) for the blends at low PEVA content (<50 wt %) was not observed. This phenomenon was also observed by different authors using other polymeric systems.²⁴⁻²⁸ This fact may be explained in terms of thermodynamic mixing accompanied by the exothermic interaction between a crystalline polymer and an amorphous polymer.

A quantitative evaluation of the T_g -composition relationship of a miscible blend may provide some tips for the blend homogeneity scale. Table II is also showing an elevation of T_g (i.e., above the additivity rule) due to the hydrogen bonding that occurred between PEVA and PEMAH blends. The intensity of these interactions was obtained from Kwei equation²⁹:

$$T_{g_m} = w_1 T_{g_1} + w_2 T_{g_2} + q w_1 w_2 \quad (1)$$

TABLE II
Thermal Properties of PEVA, PEMA, and PEVA/PEMAH Blends Obtained by DSC

System (wt %), PEVA/PEMAH	T_g^{exp} (°C) ^a	T_g^{calc} (°C) ^b	T_m (°C)	ΔH_m (J g ⁻¹)
100 : 0	55	—	167	65
95 : 5	60	59	165	38
90 : 0	70	63	163	32
85 : 15	75	67	160	27
75 : 25	85	75	148	20
50 : 50	107	95	—	—
25 : 75	125	115	—	—
10 : 90	132	127	—	—
0 : 100	135	—	—	—

^a Experimental value.

^b Calculated from the additivity rule : $w_1 T_{g_1} + w_2 T_{g_2}$.

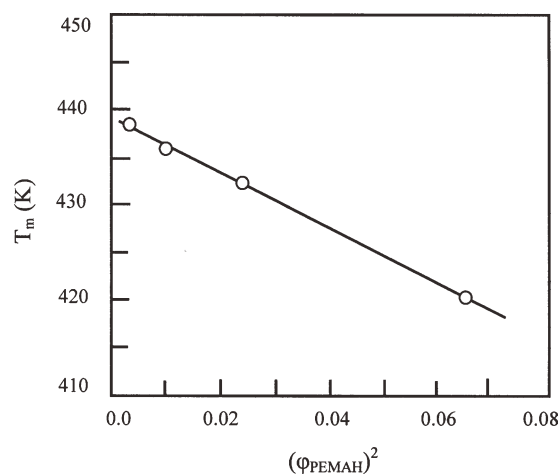


Figure 2 Melting temperature of PEVA/PEMAH blends as a function of the square of the volume fraction of PEMAH.

where w_i , T_{gi} , and T_{gm} are the weight fractions and glass transition temperatures of the constituents and mixture, respectively.

A reasonable fitting was obtained, and the best fitted parametric value was quite high at about $q = 49$, which was obtained by fitting with the entire range of the T_g -composition data. It has been suggested that the parameter (q) in Kwei equation correlates with the intensity of the interactions between the constituent molecular segments.²⁹ It is well known according to the literature^{27,30} that the relatively high value of q suggests that the molecular interaction is particularly strong or specific. This fact reflects the presence of intermolecular interactions of hydrogen bonding type between the carbonyls of maleic anhydride and hydroxyl of vinylalcohol groups of the different polymers. These interactions reduce the free volume and mobility of the polymer chains and lead to a rise in the T_g values. To estimate the intermolecular interaction between PEVA and PEMAH quantitatively, a curve of T_m versus ϕ_{PEMAH}^2 has been plotted (Fig. 2).

The thermodynamic interaction parameter ($\chi_{1,2}$) can be calculated from Nishi et al. expression.³¹

$$\Delta T_m = T_m^0 - T_m = -R \left(\frac{V_{u2}(T_m^0)^2 \chi_{1,2}}{\Delta H_{u2} V_{u1}} \right) \phi_1^2 \quad (2)$$

where the subscripts 1 and 2 designate the amorphous and crystalline polymer component, respectively, T_m^0 is the melting temperature of pure crystalline polymer (2), T_m is the melting temperature of the blend; ϕ_1 is the volume fraction of polymer (1), V_u is the molar volume of repeating units; ΔH_u is the molar enthalpy of fusion of repeating unit; and R is the gas constant. By applying eq. (2), a plot of $T_m(K)$ against ϕ_1^2 should give a straight line

with a slope of $\chi_{1,2}$ indicating that Nishi equation could describe perfectly the dynamic interaction between PEVA and PEMAH in the blend. The determination of the Flory interaction parameter ($\chi_{1,2}$) between the two polymers was possible with the data collected from the literature,^{1,4} where $\Delta H_{uPEVA} = 4.22 \text{ kJ mol}^{-1}$, $V_{uPEVA} = 37.80 \text{ cm}^3 \text{ mol}^{-1}$, and $V_{uPEMAH} = 60.32 \text{ cm}^3 \text{ mol}^{-1}$ calculated from the density of PEMAH and the molecular weight of 2-ethylmaleic anhydride, because this molecule constitutes the unit of PEMAH. Using these values, $\chi_{1,2}$ was estimated as -0.89 ± 0.10 . Thus, there may be comparatively strong intermolecular interactions between PEVA and PEMAH.

Thermal behavior of PEVA/PEMAH blends

The DSC cooling thermograms at different cooling rates of PEVA and PEVA/PEMAH blends have been realized and the thermograms of pure PEVA and 95, 90, and 85 wt % are shown in Figure 3. For the PEVA component, the crystallization temperature (T_p) and ΔH_c decreased on addition of PEMAH content, therefore PEVA could not be crystallized in the blend with PEMAH content superior to 15 wt %. This confirmed the miscibility between PVA and PEMAH. The addition of PEMAH made the molecular transport of PEVA segments to the crystallization front difficult and a higher supercooling was needed for crystallization. It also limited the thickening and perfection of the PEVA crystals, causing a depression of T_m and T_p . In all cases, in general, the crystallization enthalpy peak shifted to a lower temperature with an increasing cooling rate. Therefore, the lower the cooling rate, the easier the crystallization. All the temperature peaks of the blends were lower than the crystallization peak of PEVA. A similar shift of the crystallization peak to a lower temperature has also been reported by different authors using poly(acetostyrene)/poly(ethylene oxide) blend²⁶ and poly(ϵ -caprolactone)/epoxy resin blend.³² They suggested that the dispersed phase of amorphous polymer acted as a weak nucleating agent.

Nonisothermal crystallization kinetics of PEVA and PEVA/PEMAH blends

The influence of dispersed PEMAH on the nonisothermal crystallization kinetics of PEVA was considered. As shown in Figure 4, the peak crystallization temperature (T_p) corresponding to the crystallization enthalpy peak was lower at a relatively higher PEMAH content. In this respect, the effect of PEMAH contents <10% was not significant. When the specimens were cooled down at a high cooling rate, the motion of PEVA molecular chains seemed not to follow the cooling temperature in time due to

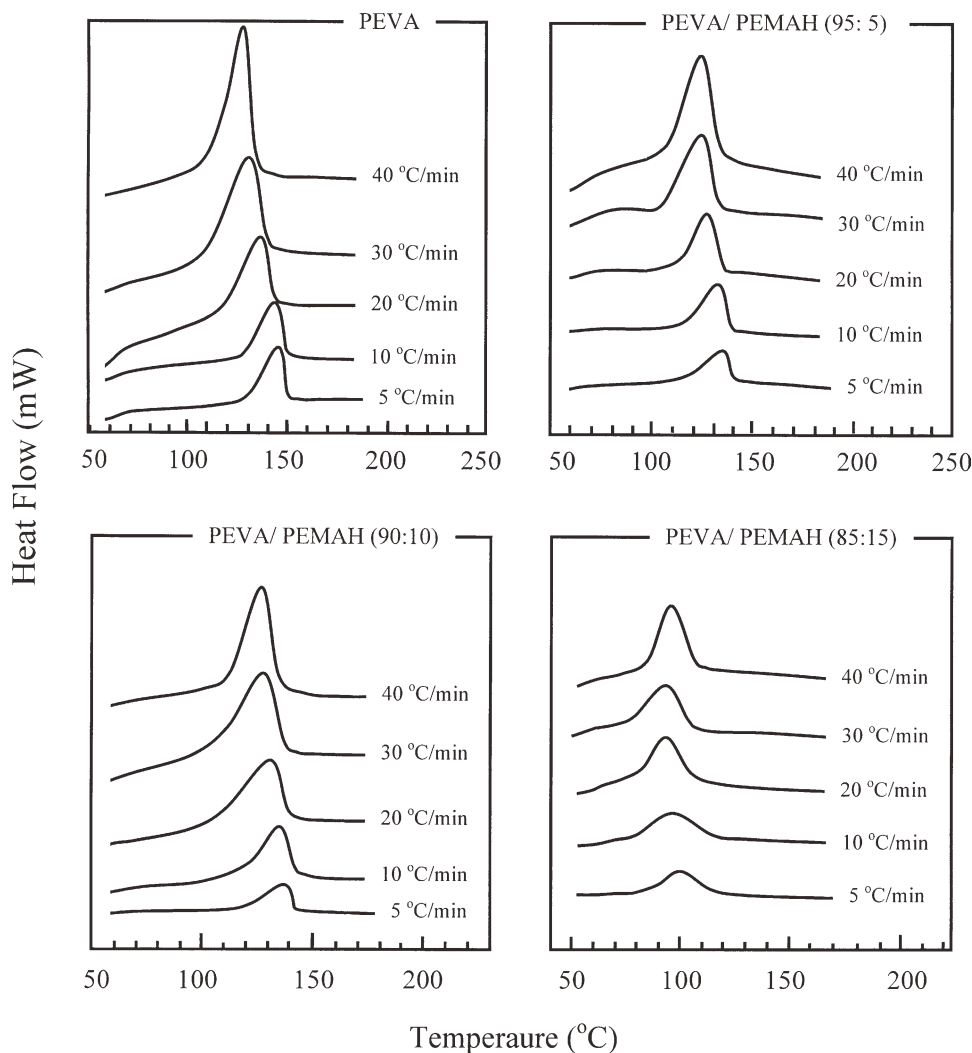


Figure 3 DSC thermograms of pure PEVA and PEVA/PEMAH blends (wt %) at different cooling rates.

the influence of heat hysteresis, which led to a lower peak crystallization temperature. When PEMAH was added into the PEVA matrix, the molecular chains of PEMAH acted as a heat barrier preventing the heat transfer among the PEVA molecular chains and consequently crystallization occurred at a lower temperature when the PEMAH content was high.

The relative degree of crystallinity, X_T , as a function of crystallization temperature can be obtained from the following equation.³³

$$X_T = \frac{A_T}{A_\infty} \quad (3)$$

where A_T is the area under the DSC curves from $T = T_0$ to $T = T$ and A_∞ is the total area under the crystallization curve. Based on this equation, X_T at a specific temperature can be calculated. Integration of the exothermic peaks during the nonisothermal scans gave a relative degree of crystallinity (X_T) as a function of temperature for PEVA and PEVA/

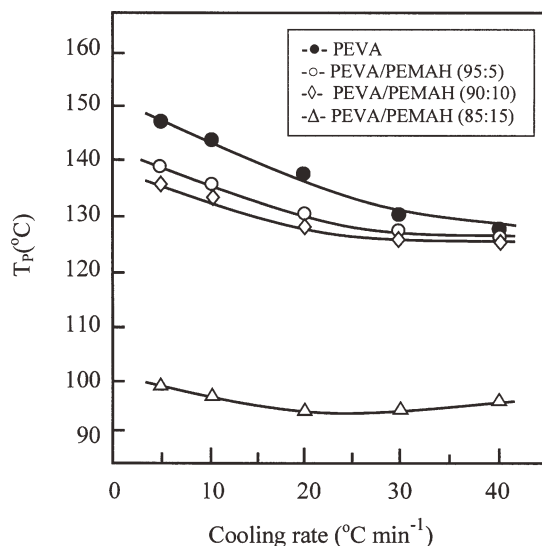


Figure 4 Relation between T_p and cooling rate.

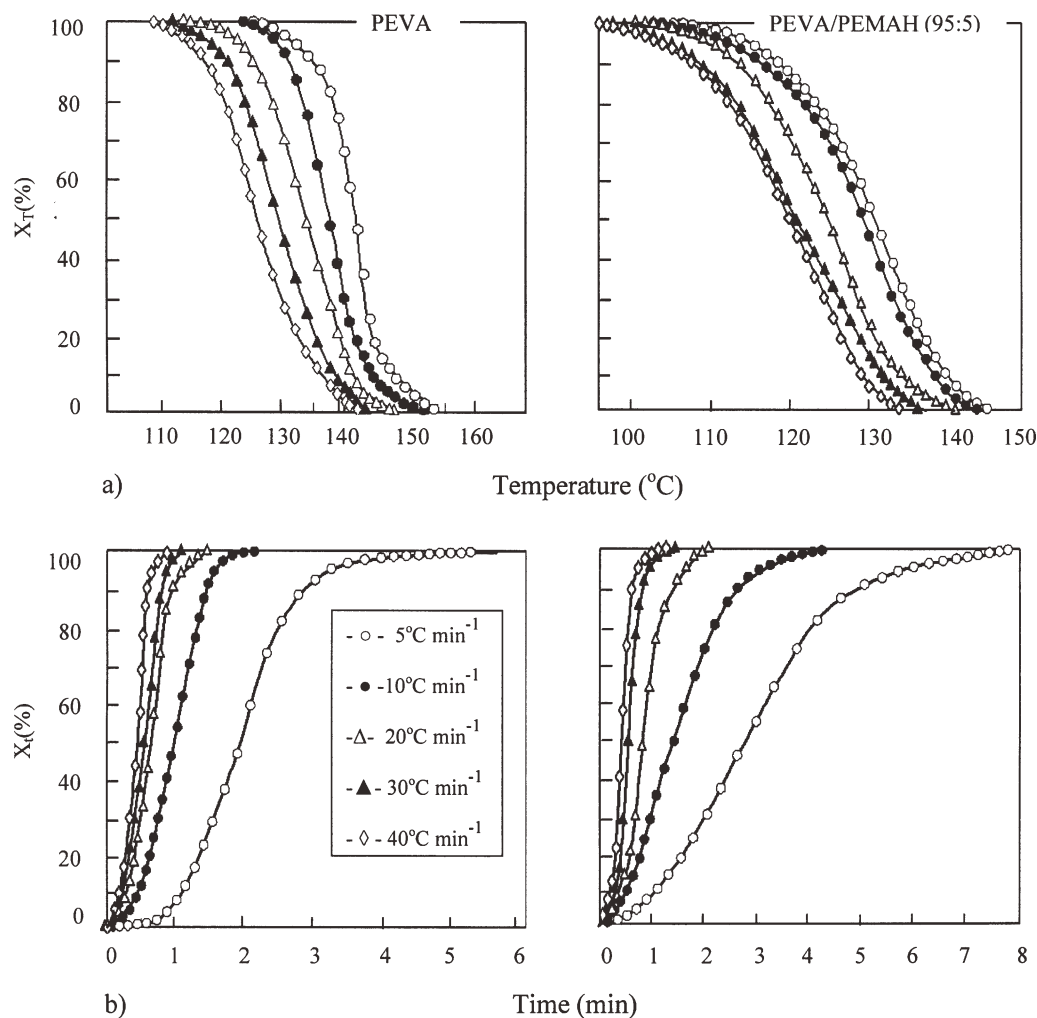


Figure 5 (a) Dependence of X_T on the crystallization temperature and cooling rate and (b) dependence of X_t on the crystallization time and cooling rate.

PEMAH blends. Figure 5(a) shows the variation of X_T versus the temperature for pure PEVA and the blend at 95 wt % of PEMAH content. Because of the effect of retardation on crystallization, all curves have approximately sigmoid patterns.

During nonisothermal crystallization, the variation of the crystallization time as the crystallization temperature obeys the following equation:

$$t = \frac{(T_0 - T)}{\beta} \quad (4)$$

where T is the temperature at crystallization time t , and β is the cooling rate.

A typical plot of X_t versus time for PEVA and the same blend traced using the combination of equations [eqs. (3) and (4)] is shown in Figure 5(b). As in case of plots X_T versus temperature, all curves of PEVA and blends have approximately sigmoid patterns and the slopes of the curves at each point were the measures of the rate of crystallization. It can be

seen that the rate of crystallization kept almost constant for 20–80% of the relative crystallinity because those parts of the curves were almost straight. At a later stage, the curves tend to become flat due to the spherulite impingement.³⁴

The half time for completing crystallization ($t_{1/2}$) can be estimated from the curves indicating the variation of X_t versus time (Fig. 6). With an increase in PEMAH content, $t_{1/2}$ increased dramatically when the cooling rate was 5°C min^{-1} . On the other hand, at $20^\circ\text{C min}^{-1}$ a straight line was observed with a weak slope. Below this cooling rate, no significant variation was noted. This observation could be explained by the fact that at a relatively low PEMAH content, the molecules of PEMAH clusters could not restrict the motion of the PEVA molecular chains, but acted as a heterogeneous nucleating agent during the nonisothermal crystallization process and therefore accelerated the crystallization. At a higher PEMAH content, the molecular chains of PEMAH clusters acted as a barrier that restricted the

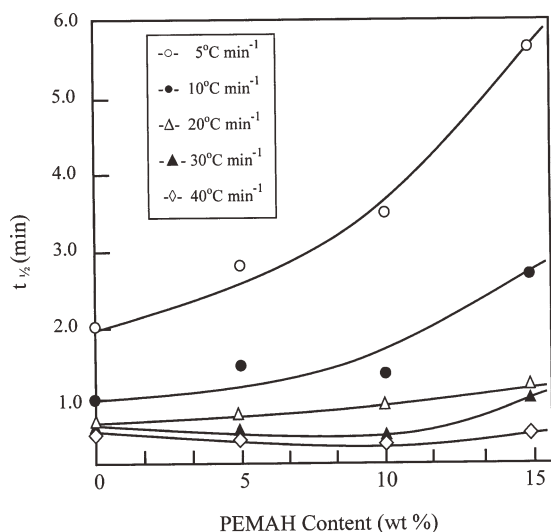


Figure 6 Variation of $t_{1/2}$ with PMAH content at various cooling rates.

thermal motion of PEVA molecular chains and therefore retarded the formation of crystals. As a result, the addition of a large amount of PMAH could delay the overall crystallization process.

Although many models have been developed for isothermal crystallization kinetics, only the models from Jeziorny,³⁵ Ziabicki,^{36,37} and Ozawa³⁴ are suitable for nonisothermal kinetics. In this study, the Ozawa relationship,

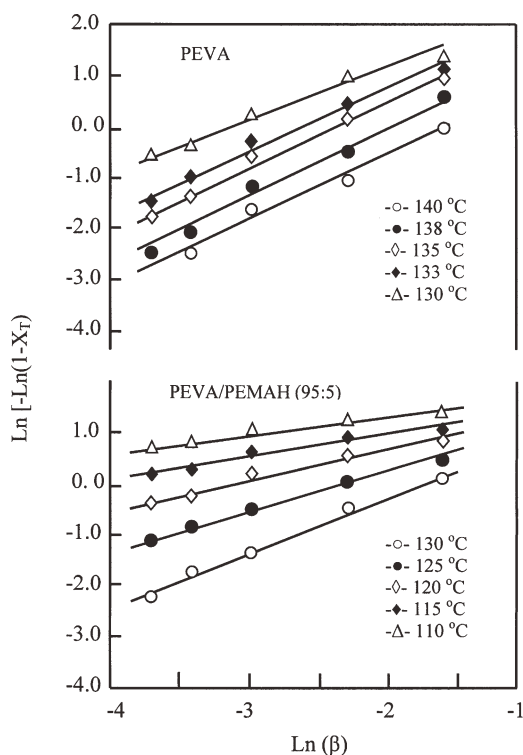


Figure 7 Ozawa plots of $\ln[-\ln(1 - X_T)]$ versus $-\ln(\beta)$ for PEVA and PVA/PEMAH (95 : 5 wt %).

$$1 - X_T = \exp\left(-\frac{k_T}{\beta^m}\right) \quad (5)$$

or

$$\ln[-\ln(1 - X_T)] = \ln k_T - m \ln \beta \quad (6)$$

where m is the Ozawa exponent depending on the dimension of crystal growth was adopted to investigate the nonisothermal crystallization of the pure polymer and the blend at various cooling rates. According to the literature,^{23,38-40} the Ozawa equation is an extension of the Avrami⁴¹ relationship to the nonisothermal condition, by assuming that nonisothermal crystallization process may be composed of infinitesimally small isothermal crystallization steps,

$$1 - X_t = \exp(-kt^n) \quad (7)$$

where X_t and X_T are the relative degrees of crystallinity as a function of crystallization time and temperature respectively, k is the constant of crystallization kinetics rate, k_T is the cooling function of nonisothermal crystallization at temperature T , t is the crystallization time, β is the cooling rate, and n is the isothermal Avrami exponent. Plots of $\ln[-\ln(1 - X_t)]$ versus $\ln(\beta)$ of PEVA and PEVA/PEMAH blends of all samples at 95, 90, and 85 wt % PEVA content showed a straight line (Fig. 7) indicating that the Ozawa equation [eq. (5)] could describe perfectly the primary process of nonisothermal crystallization of PEVA and PEVA/PEMAH blends. The intercept and

TABLE III
Ozawa Parameter (m), Cooling Function (K_T) and Half-Time ($t_{1/2}$) for PEVA and PEVA/PEMAH Blends

Sample	T (°C)	m	K_T
PEVA	140	1.41	10.42
	138	1.54	24.20
	135	1.45	32.50
	132	1.36	37.50
	130	1.22	41.70
PEVA/PEMAH (95 : 5)	130	0.95	4.17
	125	0.88	7.33
	120	0.77	10.67
	115	0.64	11.31
	110	0.50	11.59
PEVA/PEMAH (90 : 10)	135	0.45	0.28
	133	0.41	0.44
	130	0.36	0.76
	128	0.32	1.07
	125	0.33	1.52
PEVA/PEMAH (85 : 15)	120	0.32	2.82
	100	0.59	0.91
	95	0.60	0.94
	90	0.48	2.80
	85	0.50	4.48
	80	0.51	8.44

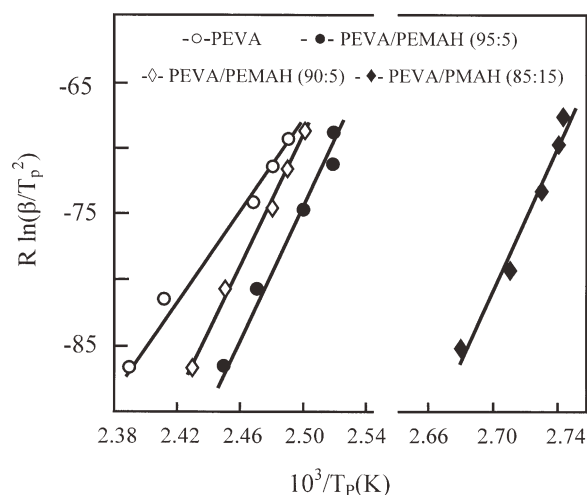


Figure 8 Variation of $\ln(\beta/T_p^2)$ versus $1/T_p$ for pure PEVA and PEVA/PEMAH blends.

slope of $\ln[-\ln(1 - X_T)]$ versus $\ln(\beta)$ yielded the crystallization kinetics rate (k_T) and the Ozawa exponent (m), respectively. The results of m and k_T of PEVA and PEVA/PEMAH blends are gathered in Table III. It could be read from these data that the value of m for PEVA was practically constant with the crystallization temperature (1.40 ± 0.20). This result was close to the value reported in the literature,⁴² while the value of m for PEVA/PEMAH (95 : 5) and PEVA/PEMAH (90 : 10) blends increased from 0.32 to 0.95 and stabilized at 0.54 ± 0.06 for the blend at 85 wt % PEVA content, which was obviously lower than that of PEVA, suggesting that the introduction of PEMAH content in PEVA matrix greatly influenced the growth of crystals. The increasing m values were usually attributed to the change from instantaneous to sporadic nucleation.⁴³ The k_T for PEVA and PEVA/PEMAH blends was unstable; it decreased significantly from 41.70 to 10.43, 11.59 to 4.17, 2.82 to 0.28, and 8.44 to 0.91 for pure PEVA, 95%, 90%, and 85% PEVA in the blends, respectively. The fluctuation of m and k_T for the blends could be attributed to the complexity of dynamic crystallization process as a function of crystallization time and temperature.

The crystallization activation energy (E_c) associated with the overall process of crystallization has been evaluated from the rates of crystallization by using the Kissinger⁴⁴ equation [eq. (8)].

$$E_c = \frac{d[\ln(\beta/T_p^2)]}{d(1/T_p)} R \quad (8)$$

where R is the universal gas constant and T_p is the peak crystallization temperature.

Plotting $R \ln(\beta/T_p^2)$ versus $1/T$ and E_c was obtained from the slope (Fig. 8). It was found that the crystallization activation energy was 186 ± 15 kJ for pure PEVA and 254 ± 15 , 267 ± 10 , and $283 \pm$

12 kJ, respectively, for the blends at 5, 10, and 15% PEMAH content. It was easy to note that the E_c of the blends increased when PEMAH content increased. This result may be explained by the miscibility of PEVA with PEMAH chains. Increasing the PEMAH content in the blends resulted in both dilution of PEVA chains at the crystal growth front and reduction of mobility of the PEMAH chains due to the higher T_g of the blend than that of pure PEVA and hence caused a higher E_c value for PEVA crystallization in the blends.

CONCLUSION

The miscibility of PEVA/PEMAH blend in all proportions in DMF was proved by viscosimetry using Krigbaum–Wall approach from the positive Δb_{23} . The differential scanning analysis confirmed the miscibility in all proportions of this system by the presence of only one glass transition temperature, intermediate between those of the two pure constituents. By using the Kwei approach, it also allowed to confirm the miscibility of the system by the existence of specific interactions between the hydroxyl groups of PEVA and the carbonyl groups of PEMAH. The miscibility of this system was also confirmed by decreasing T_p , T_m , crystallinity, and crystallization rate of PEVA in PEVA/PEMAH blends. The chains of PEMAH were uniformly distributed throughout PEVA matrix. At a low PEMAH content, the crystallization of the blend was accelerated, while at a higher content, its crystallization was retarded. The crystallinity degree of the blends decreased with an increasing PEMAH content, but increased with the cooling rate. The peak crystallization temperature decreased with the cooling rate and PEMAH content. The Ozawa parameter m and cooling function k_T of the blends changed with the crystallization temperature and addition of PEMAH. The crystallization activation energy of PVA/PMAH increased dramatically when PEMAH content increased.

The authors extend their appreciation to the Deanship of Scientific Research at King Saud University for funding the work through the research group project No. RGP-VPP-025.

References

1. Young, T. H.; Lai, J. Y.; You, W. M.; Cheng, L. P. *J Membr Sci* 1997, 128, 55.
2. Montoya, M.; Abad, M. J.; Bara, L.; Bernal, C. *Eur Polym J* 2006, 42, 265.
3. Keskin, S.; Elliot, J. R. *Ind Eng Chem Res* 2003, 42, 6331.
4. Akiba, I.; Akiyama, S. *Polym J* 1994, 26, 837.
5. Ahn, S. B.; Jeong H. M. *Polymer (Korea)* 1999, 23, 837.
6. Katime, I.; Parada, L. G.; Meaurio, E.; Cesteros, L. C. *Polymer* 2000, 41, 1369.
7. Parada, L. G.; Meaurio, E.; Cesteros, L. C.; Katime, I. *Macromol Chem Phys* 1998, 199, 1597.

8. Lv, R.; Zhou, J.; Du, Q.; Wang, H.; Zhong, W. J. *J Membr Sci* 2006, 281, 700.
9. Faisant, J. B.; Ait-Kadi, A.; Bousmina, M.; Deschenes, L. *Polymer* 1998, 39, 533.
10. Lee, C. M.; Kim, E. S.; Yoon, J. S. *J Appl Polym Sci* 2005, 98, 886.
11. Akiba, I.; Akiyama, S. *Polym J* 1994, 26, 873.
12. Jiang, W.; Qiao, W.; Sun, K. *Carbohydr Polym* 2006, 65, 139.
13. Samios, C. K.; Kalfoglou, N. K. *Polymer* 2001, 42, 3687.
14. Adoor, S. G.; Manjeshwar, L. S.; Krishna-Rao, K. S. V.; Naidu, B. V. K.; Aminabhavi, T. M. *J Appl Polym Sci* 2006, 100, 2415.
15. Garmabi, H.; Demarquette, N. R.; Kamal, M. R. *Int Polym Proc* 1998, 13, 183.
16. Young, L. S.; Chul, K. S. *J Appl Sci* 1998, 68, 1245.
17. Tselios, C. H.; Bikiaris, D.; Maslis, V.; Panayiotou, C. *Polymer* 1998, 39, 6807.
18. Tasso, M.; Cordeiro, A. L.; Salchert, K.; Werner, C. *Macromol Biosci* 2009, 9, 922.
19. Soria, V.; Gomez, C. M.; Falo, M.; Abad, C.; Campos, A. *J Appl Polym Sci* 2006, 100, 900.
20. Krigbaum, W. R.; Wall, F. T. *J Polym Sci* 1950, 5, 505.
21. Torrens, F.; Soria, V.; Codoner, A.; Abad, C.; Campos, A. *Eur Polym J* 2006, 42, 2807.
22. Lewandowska, K. *Eur Polym J* 2005, 41, 55.
23. Utracki, L.A.; Favis, B.D.; Cheremisinoff, Editors, *Handbook of Polymer Science and Technology, vol. 4, Composites and Speciality Applications*, Marcel Dekker Inc., NY, (1989).
24. Lin, J. H.; Moo, E. M.; Hung, Y. P. *J Polym Sci Part B: Polym Phys* 2006, 44, 3357.
25. Habi, A.; Djadoun, S. *Eur Polym J* 1999, 35, 483.
26. Hsu, W. P. *J Appl Polym Sci* 2002, 83, 1425.
27. Guo, Q.; Groeninckx, G. *Polymer* 2001, 42, 8647.
28. Alvarez, V. A.; Stephani, P. M.; Vazquez, A. *J Therm Anal Cal* 2005, 79, 187.
29. Kwei, T. *J Polym Sci* 1984, 22, 307.
30. Pratt, C. F.; Hobbs, S. Y. *Polymer* 1976, 17, 12.
31. Nishi, T.; Wang, T. T. *Macromolecules* 1975, 8, 909.
32. Guo, Q.; Groeninckx, G. *Polymer* 2001, 42, 8647.
33. Hammami, A.; Spruiell, J. E.; Mohrotra, A. K. *Polym Eng Sci* 1995, 35, 797.
34. Ozawa, T. *Polymer* 1971, 12, 150.
35. Jeziorny, A. *Polymer* 1978, 19, 1142.
36. Ziabicki, A. *Coll Polym Sci* 1996a, 274, 209.
37. Ziabicki, A.; *Coll Polym Sci* 1996b, 274, 705.
38. Shi, X. M.; Zhang, J.; Jin, J.; Chen, S. J. *eXpress Polym Lett* 2008, 2, 623.
39. Huang, H.; Gu, L.; Ozaki, Y. *Polymer* 2006, 47, 3935.
40. Kalkar, A. K.; Despande, A. A. *Polym Eng Sci* 2001, 41, 1597.
41. Avrami, M. J. *J Chem Phys* 1939, 7, 1103.
42. Alvarez, V. A.; Stephani, P. M.; Vazquez, A. *J Therm Anal Cal* 2005, 79, 187.
43. Pratt, C. F.; Hobbs, S. Y. *Polymer* 1976, 17, 12.
44. Kissinger, H. E. *J Res Natl Bur Stand (US)* 1956, 57, 217.